Received: 6 July 2017 | Accepted: 21 August 2017

DOI: 10.1111/jace.15190

RAPID COMMUNICATION

Journal of the American Ceramic Society

Blunt scratch strength of polycrystalline alumina

Robert F. Cook

Materials Measurement Science Division, National Institute of Standards and Technology, Gaithersburg, Maryland

Correspondence
Robert F. Cook, Materials Measurement Science Division, National Institute of Standards and Technology, Gaithersburg, MD.
Email: robert.cook@nist.gov

Abstract

A model for the fracture strength of brittle materials controlled by blunt (spherical) scratches is developed and compared with measurements on a polycrystalline alumina. The model is based on a residual stress-intensity factor for median cracks at scratches that include a localized plastic deformation zone formed by dragged spherical contacts. The stress-intensity factor depends nonlinearly on the normal contact load P, resulting in a predicted strength variation of $P^{-3/4}$. The strength result validates previous claims and extends the overall indentation-strength framework. However, the result has only limited effectiveness in describing experimental measurements, pertaining only to ideal blunt scratches formed over a limited load domain.

KEYWORDS

alumina, cracks/cracking, mechanical properties, strength

1 | INTRODUCTION

In a recent work,[1] the strengths of brittle materials, such as ceramics and glasses, controlled by scratch flaws were investigated within the context of a multiscale model of strength degradation by contact flaws.[2] The predominant strength variation was shown to be nonlinear in the normal contact load used to form the scratch and, for the sharp scratch flaws used, the decrease in strength with contact load varied as $P^{-1/2}$, where P is the normal contact load. Allusion was made in the scratch work[1] and earlier in a roller work[3] that the decrease in strength of components containing a *blunt* scratch, formed, for example, by a dragged spherical particle should vary as $P^{-3/4}$, a result originally attributable to Marshall [D. B. Marshall, private communication (1983)]. It is the intent of this Communication to show the development of the $P^{-3/4}$ dependence and to test the dependence experimentally. As before,[1] the test material is a polycrystalline alumina.

Figure 1A shows a schematic diagram of a linear elastic-plastic contact flaw formed by a dragged spherical contact with normal contact load P. A conospherical indenter is shown, consistent with the experiments to follow, but a dragged particle of any shape with a characteristic contact radius is consistent with the model to be developed. The dragged contact leaves a linear residual contact impression (the "track") in the surface of the material. Beneath the track, there is a (near semicylindrical) localized zone of plastic deformation. The strain mismatch between the plastically deformed material and the surrounding elastic matrix leads to a tensile tangential residual stress in the matrix beneath the plastic deformation zone.[1,3,4] This tensile field initiates and stabilizes median cracks that extend into the matrix perpendicular to the surface beneath the zone. It is these cracks that propagate to failure under the influence of a subsequent applied stress that is superposed on the residual field. The influence of the residual field on a median crack is given by a stress-intensity factor (SIF), K_w, written generally as[1]

$$K_w = \chi_w P_w / c^{1/2} \tag{1}$$

where (Figure 1B) P_w is the effective *force per length* wedging the median crack open at its mouth, c is the median crack length measured from the surface, and χ_w is a dimensionless constant characterizing the elastic-plastic stress field and the geometry of the zone and crack. The goal, as in previous works,[1,3] is to find the nonlinear relationship between the wedging load/length, P_w, acting on

the fully formed median crack and the experimentally determined or measured normal load, P, acting on the spherical contact during the formation of the track.

Figure 1B shows a cross-sectional view of the flaw and its dimensions. The track is formed by a segment of a disk of radius R that intersects the surface at full width $2w$; the cross-sectional area of material displaced by the contact to form the track is δA. The cross-sectional area of the plastic deformation zone into which the track material is displaced is A. The volume of material displaced is thus $\delta V = \delta A \cdot L$ and the volume of the plastic deformation zone is $V = A \cdot L$, where L is the length of the track. The constrained dilatation of the plastic deformation zone by the elastic matrix gives rise to a characteristic pressure, p, in the matrix that is proportional to the volume strain, and thus, the cross-sectional areal strain:

$$p = K(\delta V/V) \approx E(\delta A/A) \tag{2}$$

where K is the bulk modulus of the material, E is the Young's modulus of the material, and terms in the Poisson's ratio have been neglected. The total residual *force* exerted by the plastic deformation zone on the matrix, P_r, $= P_w \cdot L$, is proportional to this pressure and the side elevation area of the plastic deformation zone, $A^{1/2} \cdot L$ (to first approximation, $A^{1/2} \approx w$). Hence

$$P_r \approx pA^{1/2}L \tag{3}$$

and thus, combining Equations (2) and (3) and dividing by L, the force per length that appears in the residual SIF driving the median crack, Equation (1), is given by

$$P_w \approx E(\delta A/A)^{1/2}(\delta A)^{1/2} = E(\delta A/A)^{1/2} R\left[\cos^{-1}\sqrt{1-(w/R)^2} - (w/R)\sqrt{1-(w/R)^2}\right]^{1/2} \tag{4}$$

where the last term on the right side of the second line represents the area of the segment of a disk and can be obtained by simple integration. As before,[1,3,4] an equivalence principal is now used to equate the width of the supported area *during* the formation of the track by a translating spherical contact to the width of a residual impression remaining *after* indentation by a literal wedge. In both cases, the mean supported contact stress, the hardness H, is identical and in the case of the translating spherical contact,

$$P = \pi w^2/2H \tag{5a}$$

where it is recognized that only the front half of sphere supports the applied normal load (similar to the rolling cone[3] or translating pyramid[1]). It is convenient to define a limiting load P_R as

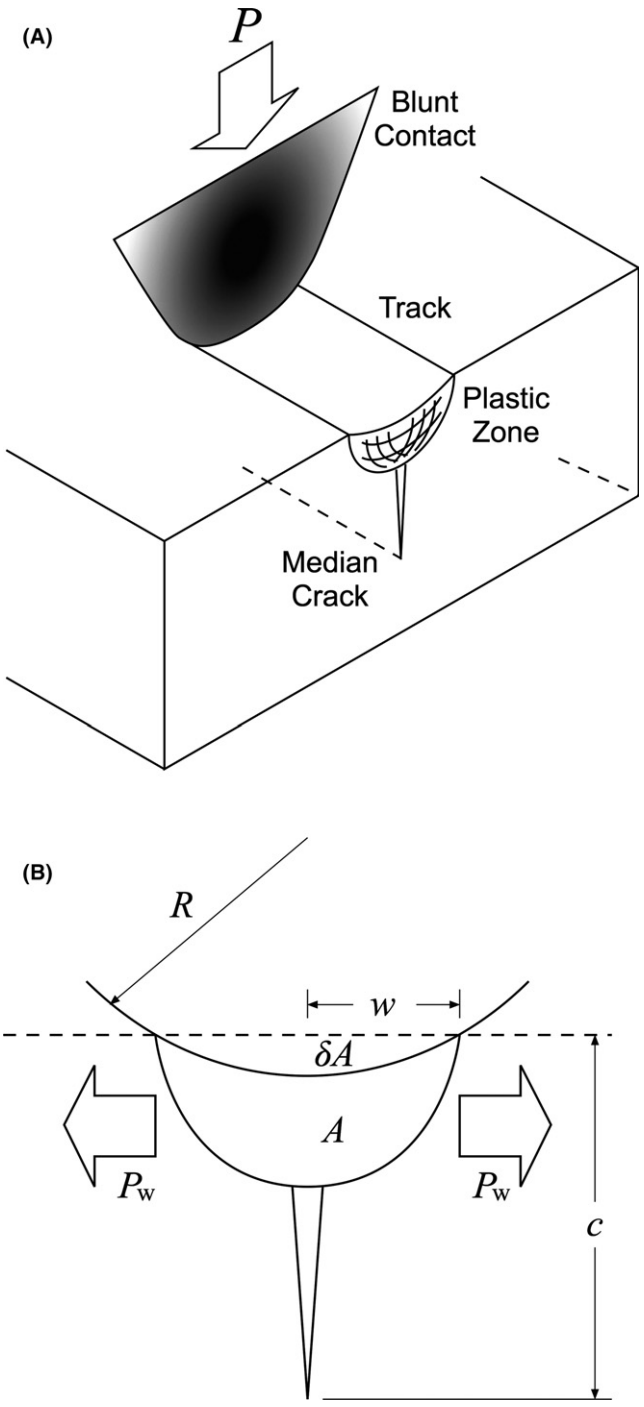

FIGURE 1 (A) Schematic diagram of a blunt spherical contact forming a scratch in the surface of a brittle material. The contact, under normal load P, leaves a surface track along with a subsurface plastic deformation zone and median crack. (B) Schematic cross-section of a spherical scratch track. The radius of the contact, R, and the resulting width, $2w$, are shown along with the cross-sectional areas of the track and plastic deformation zone, δA and A, respectively. The strain in the plastic deformation zone results in a wedging force/length, P_w, acting on a median crack, length c

$$P_R = \pi R^2/2H \tag{5b}$$

and thus, inserting Equations (5a) and (5b), Equation (4) becomes

$$P_w \approx E(\delta A/A)^{1/2} R\left[\cos^{-1}\sqrt{1-(P/P_R)} - (P/P_R)^{1/2}\sqrt{1-(P/P_R)}\right]^{1/2} \quad (6)$$

A dimensionless logarithmic plot shows that the last term in Equation (6) varies as $(P/P_R)^{3/4}$ and hence $P_w \approx P^{3/4}$ and, from Equation (1),

$$K_{sphere} = \chi_{sphere} P^{3/4}/c^{1/2} \quad (7)$$

as stated.[1,3] As per Equations (6) and (7), χ_{sphere} is a constant that takes into account the material properties of elastic modulus (E) and plastic yield strain ($\delta A/A$), the indenter radius (R), and crack geometry.

The strength of a component containing a dominant blunt scratch flaw follows simply from previous indentation-strength formulations.[1-4] A uniform stress, σ_a, applied to a crack in a component results in an applied SIF of $K_a = \psi\sigma_a c^{1/2}$, where ψ is a dimensionless geometry term. The net SIF, K, for a median crack at a blunt scratch under the influence of an applied stress is the sum of the residual and applied SIFs: $K = K_{sphere} + K_a$. The fracture equilibrium condition is $K = T_{inert}$, where T_{inert} is the toughness of the material in an inert environment. The fracture instability condition is $dK/dc = dT_{inert}/dc = 0$. Hence, equilibrium gives

$$\chi_{sphere} P^{3/4}/c^{1/2} + \psi\sigma_a c^{1/2} = T_{inert} \quad (8a)$$

and instability gives

$$\chi_{sphere} P^{3/4}/c^{1/2} - \psi\sigma_a c^{1/2} = 0 \quad (8b)$$

Simultaneous solution of Equations (8a) and (8b) gives the maximum sustainable applied stress—the strength, σ_{max}—of the component,

$$\sigma_{max} = T_{inert}^2/4\psi\chi_{sphere} P^{3/4} \quad (9)$$

as also stated.[1,3]

Figure 2 shows the inert strength of polycrystalline alumina samples containing blunt scratch flaws formed at the normal loads indicated (0.1 N to 10 N). The scratch flaws were formed using a Rockwell C tungsten carbide spherical-tipped conospherical indenter translated under load across the sample surfaces at approximately 0.5 mm s^{-1}. The scratch length was 5 mm. The samples were 32 mm × 32 mm squares, 0.65 mm thick. The material, test-rig geometry, and inert biaxial strength-test methodology are described elsewhere.[1] The symbols in Figure 2 represent individual strength measurements. Every sample was checked by optical microscopy to ascertain failure from the introduced scratch flaw. The solid line in Figure 2 represents the $P^{-3/4}$ strength variation given above. The line has been placed to intersect the P = 3 N data and, as such, nearly intersects the P = 2 N and P = 5 N data. Without further interpretation, the model above can only be said to do a fair job of describing strength degradation by the full range of blunt scratch flaws in this polycrystalline alumina.

At large and small contact loads, the strengths in Figure 2 deviate from the "ideal" blunt scratch response. Such deviations are the norm in brittle materials. At large (>3 N here) loads, lateral cracks and chipping at the scratch decouple the plastic deformation zone from the restraining matrix, thereby reducing the residual field acting on the median cracks. As a consequence, a greater applied stress is required to maintain fracture equilibrium and cause instability, resulting in a greater strength than ideal, as observed. At small (<3 N here) loads, microstructural bridging effects behind the crack tip decrease in number and effect, thereby reducing the toughness of the material through which the median cracks are propagating. As a consequence of this effect, a smaller applied stress is required to maintain fracture equilibrium and cause instability, resulting in a smaller strength than ideal, as observed. Both of these effects were observed in much the same load range in the sharp scratch study that used the same material[1] and at larger loads in indentation studies on a range of ceramics.[1,2]

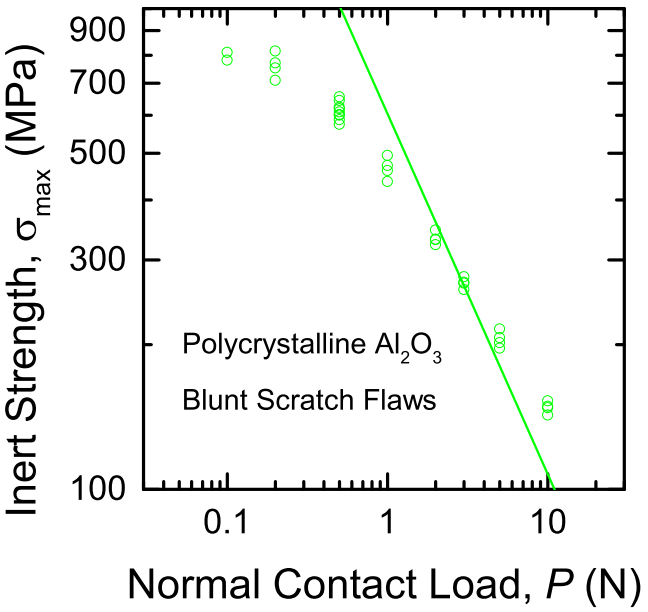

FIGURE 2 Plot of inert strength, σ_{max}, vs normal contact load, P, for blunt, spherical scratch flaws in the surface of a polycrystalline alumina. Symbols represent individual strength measurements; solid line represents the $P^{-3/4}$ trend for ideal blunt scratches [Color figure can be viewed at wileyonlinelibrary.com]

Future applications of blunt scratch strength testing will then require a fracture mechanics framework extended from that here by the addition of a microstructurally based SIF, K_μ, dominant at short crack lengths ($\sim c^{-1/2}$), and modification of K_{sphere} to include stress relief ($\sim P^{3/4}$) at large contact loads. The framework and analysis would then develop as for sharp scratch flaws,[1] yielding a similar sigmoidal inert strength variation (and as observed here). Environmental effects are expected to enter in three well-known ways. First, atmospheric moisture reduces material toughness, $T_{moisture} < T_{inert}$ (Equation 8a).[2] Second, the reduction in toughness exacerbates lateral cracking and residual stress relief, further reducing K_{sphere}.[1,2] Third, environmental reaction kinetics lead to stressing rate effects via K_a.[2,4] Hence, blunt scratches would appear to offer the prospect of extending controlled-flaw strength testing into linear flaws using the same fracture mechanics and environmental considerations as indentation flaws,[2] but without some of the issues associated with the ultra-small loads required for sharp scratches.[1]

2 | CONCLUSIONS

A fracture mechanics formulation has been developed to describe the strength degradation of brittle materials by scratches formed by blunt (spherical) contacts. The formulation is based on conventional indentation fracture mechanics[2] with key differences in the derived form of the indentation residual stress-intensity factor that depends on the normal contact load P and crack length c as $P^{3/4}/c^{1/2}$. These differences lead to a strength dependence of $P^{-3/4}$, which compares with weaker dependencies of $P^{-1/2}$ (sharp scratch)[1] and $P^{-2/3}$ (conical roller)[3] for contacts with greater degrees of geometrical similarity. Comparison of the predicted dependence with experimental data suggests that the formulation will only pertain in midlevel normal contact load domains in which the scratch flaws are ideal. At larger and smaller contact loads, lateral crack effects and microstructural effects, respectively, lead to well-understood positive and negative deviations, respectively, from the ideal strength. Irregular (nonspherical) scratches are easily handled by the introduction of a characteristic contact radius, providing the contact generates a localized plastic deformation zone and an associated median crack. The same proviso pertains to rolling spherical contacts. At extremely large contact radii or small contact loads, the contact is predominantly elastic, the scratch cracks formed are cones or partial cones[5-7] and the current analysis does not apply (and the strength varies as $P^{-1/3}$).

ORCID

Robert F. Cook http://orcid.org/0000-0003-0422-8881

REFERENCES

1. Cook RF. Fracture mechanics of sharp scratch strength of polycrystalline alumina. *J Am Ceram Soc*. 2017;100:1146-1160.
2. Cook RF. Multi-scale effects in the strength of ceramics. *J Am Ceram Soc*. 2015;98:2933-2947.
3. Cook RF. Deformation and fracture by sharp rolling contacts. *J Am Ceram Soc*. 1994;77:1263-1273.
4. Symonds BL, Cook RF, Lawn BR. Dynamic fatigue of brittle materials containing indentation line flaws. *J Mat Sci*. 1983;18:1306-1314.
5. Lawn BR, Wiederhorn SM, Roberts DE. Effect of sliding friction on the strength of brittle materials. *J Mat Sci*. 1984;19:2561-2569.
6. Leu HJ, Scattergood RO. Sliding contact fracture on glass and silicon. *J Mat Sci*. 1988;23:3006-3014.
7. Park D-S, Danyluk S, Mcnallan MJ. Friction and wear of single-crystal silicon at elevated temperatures. *J Mat Sci*. 1991;26:1505-1511.

How to cite this article: Cook RF. Blunt scratch strength of polycrystalline alumina. *J Am Ceram Soc*. 2018;101:16–19. https://doi.org/10.1111/jace.15190